Acta Mechanica Sinica (2012) 28(5):1323–1330
DOI 10.1007/s10409-012-0030-x

RESEARCH PAPER

The effect of agglomerate on micro-structural evolution in solid-state sintering

Chao Wang · Shao-Hua Chen

Received: 8 August 2011 / Revised: 2 December 2011 / Accepted: 19 December 2011

Abstract Discrete element method (DEM) is used in the present paper to simulate the microstructural evolution of a planar layer of copper particles during sintering. Formation of agglomerates and the effect of their rearrangement on densification are mainly focused on. Comparing to the existing experimental observations, we find that agglomerate can form spontaneously in sintering and its rearrangement could accelerate the densification of compacts. Snapshots of numerical simulations agree qualitatively well with experimental observations. The method could be readily extended to investigate the effect of agglomerate on sintering in a three-dimensional model, which should be very useful for understanding the evolution of microstructure of sintering systems.

Keywords Solid-state sintering · Discrete element method · Agglomerate · Densification · Micro-structural evolution

1 Introduction

To predict and even control the microstructural evolution has become a very important issue in the field of sintering research because it determines essentially the mechanical and material properties of sintered products. As we know, in the initial stage of solid-state sintering, asymmetrical neck formation can yield local forces, which may cause rotation and translation movement of particles. This process is usually addressed as particle rearrangement. Particle rearrangement has been found to be one of the crucial phenomena in sintering experiments [1], which has attracted many scientists' interests [2–14]. For example, Petzow et al. [1] attributed particle rearrangement in the planar layer of uniform copper spheres to the asymmetrical neck formation, while Weiser et al. [12] proved that differential densification was the major reason causing particle rearrangement. The influences of particle rearrangement on the average coordination number, average contact area and macroscopic stress for closed die compaction and isostatic compaction were studied by Martin et al. [13]. The other macroscopic properties influenced by particle rearrangement, such as densification rate, bulk and shear viscosity, were considered by Henrich et al. [7] and Jagota et al. [14]. Wonisch et al. [6] investigated the development of anisotropy induced by particle rearrangement. On the other hand, due to random packing, particles in the dense particle region get together more closely so that agglomerates will be produced [1, 15–17]. Since particle rearrangement is dominated by local forces, it is reasonable to assume that agglomerate rearrangement is also induced by the asymmetrical forces acting on each agglomerate. Agglomeration of particles has been observed and studied in many experiments [1, 18–20] and simulations [21, 22]. Petzow et al. [1] observed agglomeration during sintering of planar arrays of uniform copper spheres at 1 223 K. Similar phenomena have been found in irregular arrays of glass spheres [23], copper particles [12], compacts of fine tungsten powder [24], fine chromium oxide powder compacts [24] and alumina powder compacts [25]. Agglomeration occurs much more frequently during sintering of nanoparticles. Kuo et al. [19] found that almost all the powder of alumina-8vol% zirconia gets together with various sizes from less 1 μm to more than 10 μm after calcination at 823K for 2 hours. Palmero et al. [20] found a heterogeneous microstructure consist-

The project was supported by the National Natural Science Foundation of China (10972220, 11125211 and 11021262) and 973 Project (2012CB937500).

C. Wang · S.-H. Chen (✉)
State Key Laboratory of Nonlinear Mechanics,
Institute of Mechanics,
Chinese Academy of Sciences,
100190 Beijing, China
e-mail: chenshaohua72@hotmail.com

ing of agglomerates of ultrafine alumina particles with size 150 nm–200 nm, which was sintered at 1 408 K. Kadusnikov et al. have carried out several works [26–28] on agglomeration simulation using a sphere-polyhedron model. Ciftcioglu et al. [18] investigated the effect of agglomerate strength on sintered density experimentally and made a conclusion that the sintered density of yttria powders decreased with increasing agglomerate strength. Martin et al. [21] studied the morphology and strength of agglomerates through computer simulation and found that morphology of agglomerates has a clear effect on the tap density but the strength of agglomerates is a predominant factor affecting green density. However, in the studies by Ciftcioglu et al. [18] and Martin et al. [21], agglomerates were introduced into particle systems before sintering/compaction. Agglomerate rearrangement was considered by Kim et al. [22] who investigated the effect of multi-level particle packing on the packing density. In their model, particles are packed to make agglomerates, which are called as clusters and treated as big "particles". They found that systems with rearranged agglomerates have a higher packing density than those without rearrangement.

From above literatures, it should be noted that agglomerates were presupposed in the initial sintering particle systems, which, however, should form naturally and spontaneously during sintering. What is the forming process of agglomerates? What effects will be exhibited on the dynamic microstructural evolution due to the existence of agglomerates?

In the present paper, a two-dimensional sintering model for a planar layer of copper particles is considered to answer the above questions, which is similar to the experiment carried out in Ref. [1]. The concept of agglomeration used in the simulation is given first so that agglomerates are produced spontaneously during the sintering simulations. Not only the effect of particle rearrangement but also that of agglomerate rearrangement on the microstructural evolution is evolved simultaneously. The effect of agglomerate rearrangement can be abstracted from comparisons of the result with both effects of agglomerate and particle rearrangements and that only with the effect of particle rearrangement. The findings in this paper should be very useful for understanding the influence of agglomerates on microstructural evolution and densification in sintering and the method proposed in the present paper should be readily extended to a three-dimensional case.

2 Numerical simulation method

2.1 Discrete element method

The discrete element method is used to simulate the sintering process, in which the quantities describing a particle consist of a position vector $\boldsymbol{x}_i$, velocity $\dot{\boldsymbol{x}}_i$, acceleration $\ddot{\boldsymbol{x}}_i$ and mass m_i. At each time step Δt, the interacting force between two contacting particles is $\boldsymbol{F}_{ij}$, under which the acceleration $\ddot{\boldsymbol{x}}_i(t)$, velocity $\dot{\boldsymbol{x}}_i(t+\Delta t)$ and position $\boldsymbol{x}_i(t+\Delta t)$ can be calculated using the Newton's second law and a verlet type algorithm as follows,

$$\ddot{\boldsymbol{x}}_i(t) = \frac{1}{m_i}\sum_{j\neq i}\boldsymbol{F}_{ij}, \tag{1a}$$

$$\boldsymbol{x}_i(t+\Delta t) = \boldsymbol{x}_i(t) + \left(\dot{\boldsymbol{x}}_i(t) + \frac{1}{2}\ddot{\boldsymbol{x}}_i(t)\Delta t\right)\Delta t, \tag{1b}$$

$$\dot{\boldsymbol{x}}_i(t+\Delta t) = \dot{\boldsymbol{x}}_i(t) + \frac{1}{2}(\ddot{\boldsymbol{x}}_i(t) + \ddot{\boldsymbol{x}}_i(t+\Delta t))\Delta t, \tag{1c}$$

where Δt is such a small value that the particle i is assumed to interact only with its neighbors and can not move over the position of its neighbors. A real mass m_i requires the time step Δt to be a very small value, which in turn leads to prohibitive simulation times. In order to overcome this drawback, a special technique adopted by Refs. [7, 13, 29] will be used, in which the mass of a particle is scaled up by a factor β (a large number) so that the acceleration and velocity can be reduced by the same order of magnitude without influencing the equilibrium position of each particle. Thus, a relatively long time step can be chosen. The factor β should not be too large as analyzed by Henrich et al. [7]. Martin et al. [13] have used 10^{13} for β in their simulations. In the present simulation, we take $\beta = 10^8$ and the time step is 0.2 s.

The concept of affine transformation which has been used in literatures [7, 13, 29, 30] is not adopted in our simulations because of the strong restriction of rearrangement of particles as pointed out by Olmos [31]. The method used in the present paper is just like the one used in the original DEM work by Cundall [32] and in the granular study [33].

2.2 Interacting force between adjacent particles

Similar to Refs. [3, 4, 9, 34], the force N_s normal to the contact area of two contacting particles is

$$\begin{aligned} N_\mathrm{s} &= \frac{\pi a_\mathrm{s}^4}{8\Delta_\mathrm{b}}\frac{\mathrm{d}h}{\mathrm{d}t} - \pi\gamma_\mathrm{s}\left[4R_\mathrm{p}\left(1-\cos\frac{\psi}{2}\right) + a_\mathrm{s}\sin\frac{\psi}{2}\right], \\ \Delta_\mathrm{b} &= \frac{\Omega}{kT}\delta_\mathrm{b}D_\mathrm{b}, \end{aligned} \tag{2}$$

where $D_\mathrm{b} = D_{0\mathrm{b}}\exp(-Q_\mathrm{b}/RT)$ is a diffusion coefficient for vacancy transport on the grain boundary with thickness δ_b and activation energy Q_b, Ω is the atomic volume, k is the Boltzmann constant, T is the temperature, h is the indenting depth between two spherical particles, γ_s is the surface energy, R_p is the radius of particles, ψ is the dihedral angle, a_s is the sintering contact radius which grows up according to the Coble's model $a_\mathrm{s} = \sqrt{2hR_\mathrm{p}}$.

Equation (2) consists of grain boundary diffusion and surface diffusion, which is originally and strictly obtained by Bouvard and McMeeking [35] and Parhami and McMeeking [36] from the physics and mechanics viewpoints. The first term on the right hand side of Eq. (2) is the normal viscous force resisting the relative motion of two contacting particles, which has also been used in Refs. [2, 5–7].

The second term denotes the sintering force tending to pull two adjacent particles together. Note that the force given in Eq. (2) is suitable only for contacting particles. For non-contacting ones, there are no forces. Only if some particles move closely and contact an isolated particle, the initially isolated particle will be subjected to the sintering force.

The rotation of particles and the tangential forces between contacting particles are not included in our simulation for sake of simplicity.

2.3 Definition of agglomerate

An agglomerate is defined as an assembly of particles in which distances between contacting particles are smaller than $d_c \times 2R_p$, where d_c is a coefficient and set to 0.91 and 0.95 in our subsequent simulations, respectively. The larger the d_c is the earlier the formation of agglomerates in our simulations are.

At each time step, each particle has the same probability to be the center of an agglomerate. Therefore, they are chosen randomly with the same probability and the chosen number is equal to the total number of particles. This scheme is very similar to the method used in Monte Carlo simulations [37, 38].

When a particle P_i is chosen randomly, two steps are needed to detect an agglomerate with its center at P_i, as depicted in Fig. 1. The first step is to find the assembly of particles. Specifically, if the distance between two contacting particles is smaller than $d_c \times 2R_p$, then P_i belongs to this assembly. The second step is to truncate the assembly detected in the first step by introducing a cut-off radius r_c. The parameter r_c is used to define the dimension of agglomerate, whose value will influence the number of agglomerates in the system. Because the total number of particles in the system is given as 500, the number of agglomerates will be small if an agglomerate is defined to be too large. However, r_c can not be too small, otherwise two contacting particles will be thought as an agglomerate. We have adopted $r_c = 3R_p$, $4R_p$, $6R_p$ and $8R_p$ in the simulations and found that the size and number of agglomerates in a sintering system do not change the effect of agglomerates' rearrangement on the densification of compacts. An intermediate value of $r_c = 4R_p$ is chosen in the present paper. A possible microstructural evolution is shown schematically and intuitively in Fig. 2. It shows that without considering agglomeration particle i will be attracted by four adjacent contacting particles. Three particles are on the left side of the dashed line and one on the right side, which leads to a microstructure state "A" with the result of bond-breaking between particles i and j. However, considering the effect of agglomerate, particles on each side of the dashed line belong to two different agglomerates and the two agglomerates will approach to each other due to the attraction force between them, which leads to the microstructure state "B", a more densified structure. Actually, either particle i or j will be influenced not only by the neighboring contacting particles but also by particles in agglomerates that particle i or j belongs to. Both effects are included in our simulations.

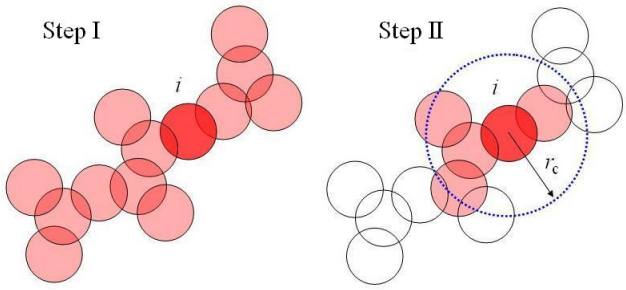

Fig. 1 Schematic of two steps for defining the assembly and agglomerate. Step I: detect the assembly to which particle i belongs; Step II: define agglomerate with a cut-off radius r_c

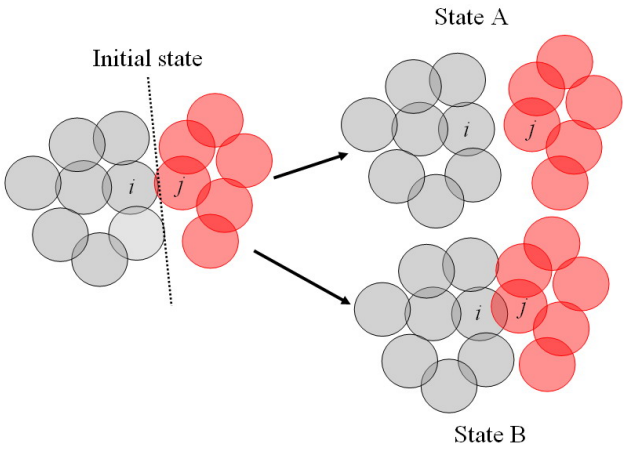

Fig. 2 Two possible microstructural evolution behaviors. State A: particle i departs from particle j without considering the effect of agglomerates; State B: coalescence of two agglomerates due to the consideration of agglomerates interaction

In DEM simulations, the interaction force between two contacting agglomerates results from the contacting particles on the boundaries of both contacting agglomerates. For example, the interaction between two agglomerates, which are labeled with different colors in Fig. 2, equals to the one between particles i and j. So, the resultant force $\boldsymbol{F}_{\text{agg}}$ acting on an agglomerate is the sum of forces exerted by the adjacent contacting particles in other agglomerates, which can be calculated by Eq. (2). The particle's acceleration in an agglomerate is then obtained as

$$\ddot{\boldsymbol{x}}_i(t) = \left(\sum_{j\neq i} \boldsymbol{F}_{ij}\right) \Big/ m_i + \boldsymbol{F}_{\text{agg}}/m_{\text{agg}}, \tag{3}$$

where m_{agg} is the mass of the agglomerate. The velocity and position of a particle in an agglomerate are updated according to Eqs. (1b) and (1c). Only the translational motion of agglomerate is considered in our simulations. The accelera-

tion of the agglomerate $\boldsymbol{F}_{\text{agg}}/m_{\text{agg}}$ is added to the acceleration of particles in it. It means that the motion of a particle in an agglomerate is affected not only by particles contacting with it but also by the agglomerate itself.

Figure 3 gives the flow chart for numerical treatment of agglomerates during our simulations.

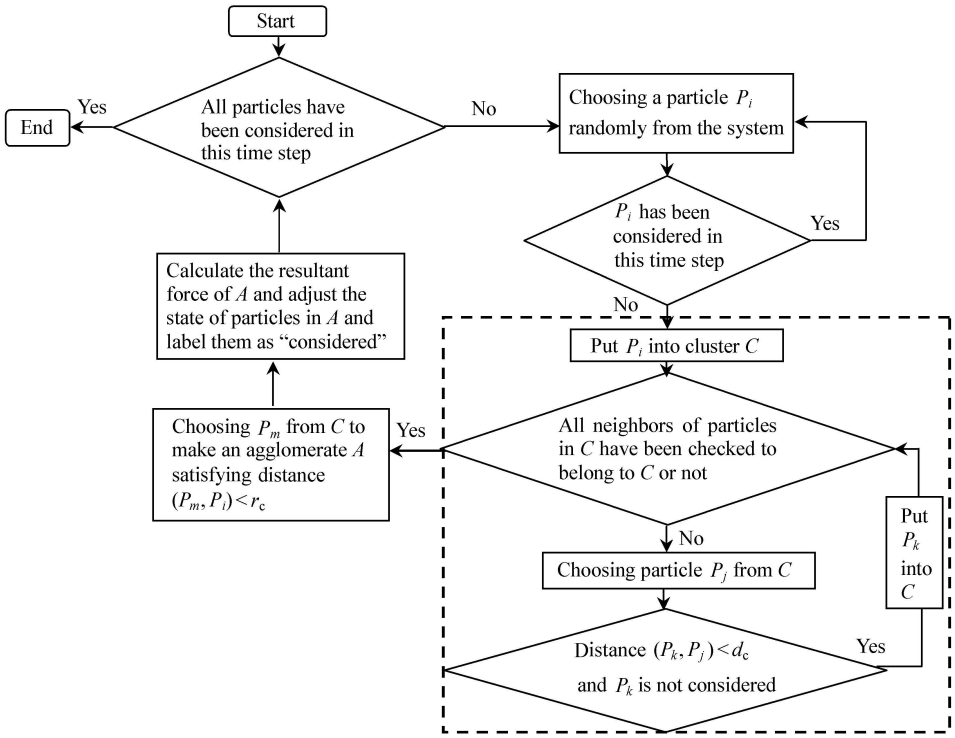

Fig. 3 The flow chart of the numerical treatment of agglomerates for simulation of sintering

3 Simulation model

Figure 4 shows a simulation model of particle system, which consists of 500 uniform copper spheres distributed in a circle region with a radius 25 times the particle radius. The initial packing fraction defined as the ratio of the sum of the projected areas of all particles to the whole circle area, which is 0.8 in the present case. Two sets of particle size and temperature are used. The first one is with the particle size of 25 μm and sintering temperature of 1 223 K, which is similar to the condition used in experiment [1] and will be used later for comparison to the experimental results. The second one is with particle size of 127 μm and temperature of 1 300 K, which is adopted for all the other simulations in the present paper. Other physical parameters used in all simulations are listed in Table 1.

Table 1 Parameters used for copper sintering in discrete element simulation (adopted from Ref. [33])

$\delta_b D_{0b}/(\mu m^3 \cdot s^{-1})$	$\psi/(^\circ)$	$Q_b/(kJ \cdot mol^{-1})$	$\gamma_s/(J \cdot m^{-2})$	Ω/nm^3
5 120	146	105	1.72	0.011 8

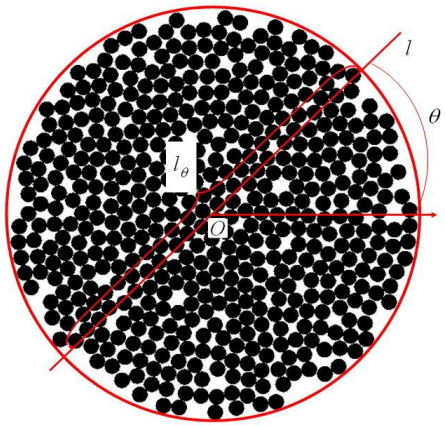

Fig. 4 Numerical simulating model with 500 uniform spheres distributed randomly in a circle region with an initial packing fraction of 0.8

Capability of the present numerical method to simulate particle rearrangement is first verified in Fig. 5. In Fig. 5a, particle rearrangement occurs significantly at the beginning

of sintering, and then decays with particles gradually adjusting their positions, as shown in Fig. 5b. Finally, all particles will move towards the center of the particle system as shown in Fig. 5c, which is well consistent with the assumption of affine transformation [31, 39].

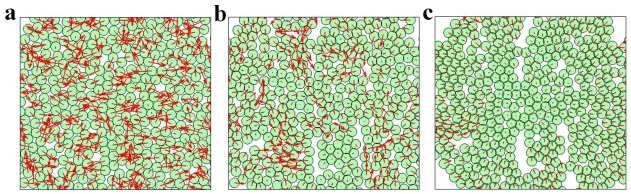

Fig. 5 Snapshots of particles' velocities in a sintering system. **a** At 5 000 time step; **b** At 5×10^5 time step; **c** At 2.5×10^6 time step. The length of each arrow is proportional to the magnitude of the particle's velocity

The above simulation results show that the assumption of affine transformation that the velocity of each particle is determined by the macroscopic strain rate is an artificially technique, which will exert a constraint on particle's initial movements. Thus, it is reasonable for us to adopt particles' initially random packing and the Newton's second law in numerical simulations of sintering.

When agglomerate rearrangement is considered, each agglomerate can be looked as a big "particle" and the force between contacting agglomerates defined in Sect. 2.3 can be used, which leads to a natural process of agglomerate rearrangement. In order to give a more intuitive understanding of agglomerate in our simulations, Fig. 6 shows the variation of the number of agglomerates as a function of the simulation time, in which the number of agglomerates increases very quickly at the initial stage, then decreases and finally tends to a constant. The varying pattern demonstrates that agglomerate forms very quickly at the initial sintering stage, and then takes part in rearrangement and grows up at the cost

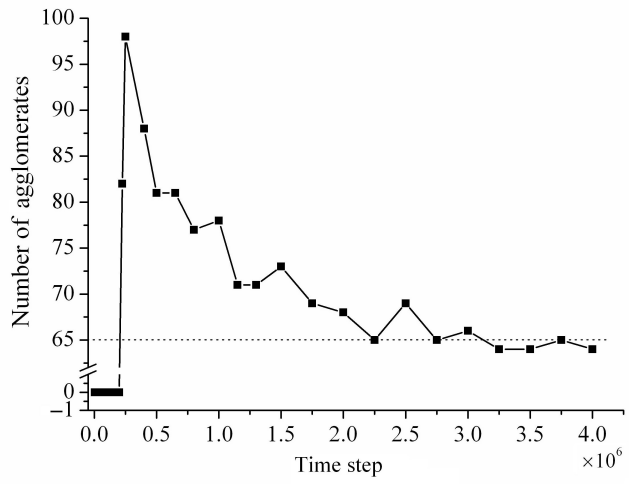

Fig. 6 The number of agglomerates as a function of simulating time steps

of its neighbors. The chosen value of cut-off radius r_c that is used to define the size of agglomerate will influence the final constant. The larger (or the smaller) the cut-off radius is, the smaller (or the larger) the final constant is.

4 Definition of characteristic parameter

The densification of the simulating system is measured by $(D_0 - D)/D_0$. Due to the irregular real boundary and some isolated particles on the boundary in the 2D system as shown in Fig. 4, it is not reasonable to characterize the densification of the system in the nominal circle area. For this reason, D and D_0 have special definitions in the present paper. As shown in Fig. 4, a straight line is used to pass through the center of the 2D system with angle θ, which is ended by two particles on the real boundary and a length l_θ can thus be measured. For θ varying from 1° to 360°, at every 1°, a length l_θ is measured, then, an average value can be found as $\bar{l} = \sum_{\theta=1^\circ}^{360^\circ} l_\theta/360$, which is regarded as the diameter of the simulating system. D_0 is the diameter at the initial time and D is the one at some sintering time.

The other parameter describing the microstructure is the average coordination number K, the definition of which is given below,

$$K = \left(\sum_i K_i\right)\Big/N, \qquad i = 1, 2, \cdots, N, \tag{4}$$

where K_i is the coordination number of particle i, N is the number of particles used in simulations.

5 Numerical results and discussions

Sintering experiment of a planar layer of uniform copper particles has been carried out by Petzow et al. [1]. In order to check the applicability of our simulation technique, comparison of numerical simulation to the experiment result [1] under similar conditions is made, in which particle size is taken as 25 μm and sintering temperature as 1 223 K. Figure 7a shows the evolution of microstructure morphologies with time steps of 5×10^5 and 7×10^5, respectively. It is found that the big pores can not be detected at the initial time and then pores emerge gradually and grow up with increasing sintering time. The simulating results of pore coarsening are qualitatively consistent with the experimental observations [1], as shown in Fig. 7b.

Pore coarsening is a result of particle agglomeration in the initial and intermediate stage of sintering. Due to the convenience of measuring porosity in experiments, variance of pore during sintering has attracted much more attentions and the microstructure evolution has always been analyzed from the pore viewpoint [16]. However, it is very difficult to describe the detailed morphology and distribution of pores,

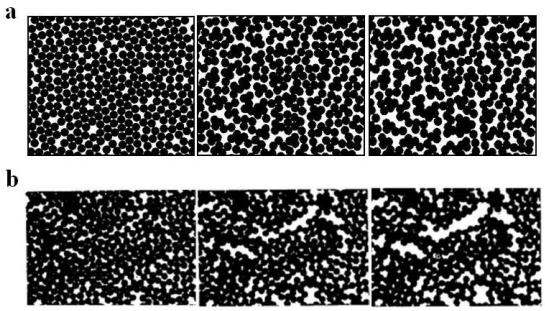

Fig. 7 Microstructural evolution and pore coarsening. **a** Snapshots in the present simulations with similar conditions to experiment [1] at three different time-steps: initial state (left), 5×10^5 time step (middle) and 7×10^5 time step (right); **b** Experimental results of planar arrays of uniform copper spheres sintering for 1 minute (left), 2 hours (middle) and 12 hours (right) at 1 223 K [1]

because they have irregular shapes and are closely interconnecting even at high relative densities. An alternative approach to analyze the microstructure evolution is from the particle point of view with discrete element method (DEM). This method could measure particles' behaviors precisely, one of which is particle agglomeration investigated in the present paper.

Variations of contact interfaces are given in Figs. 8a–8c schematically. The separation variations between two adjacent particles are expressed by white bars. An interesting phenomenon can be found that the contact interface between two particles will break at some moment and then join together again at another moment. The same phenomena have also been observed in experiments [16], as shown in Figs. 8d and 8e for comparisons. The phenomena of pore coarsening and contact breaking have been observed both in simulations considering agglomeration and in those without considering agglomeration. The difference between the two cases will be further discussed in detail as follows.

The number of new forming contact as a function of the mean coordination number of particles is given in Fig. 9 for two cases of $d_c = 0.91$ and $d_c = 0.95$. The number of new forming contacts and the coordination number is calculated at every 5 000 time steps. It shows that more contacts will form at a given coordination number when the effect of agglomerates is considered. For the case of d_c taking a value of 0.95 (agglomerates will appear earlier if d_c is bigger) as shown in Fig. 9, agglomerates will emerge when the mean coordination number gets to 2.8, and more contacts are found to form compared with the case without considering agglomerates, which provides evidence that agglomeration could enhance the densification. In addition, more contacts will form at the earlier stage of sintering when the average coordination number is relatively small, and the number of new forming contacts decreases continuously with increasing average coordination number. As the mean coordination number increases, densification proceeds and the number of adjacent particles without contacting will become fewer and fewer due to further coalescence. It also gives a more realistic sense on the rearrangement of particles. When the number of new forming contacts increases, it becomes more difficult for particles to rearrange.

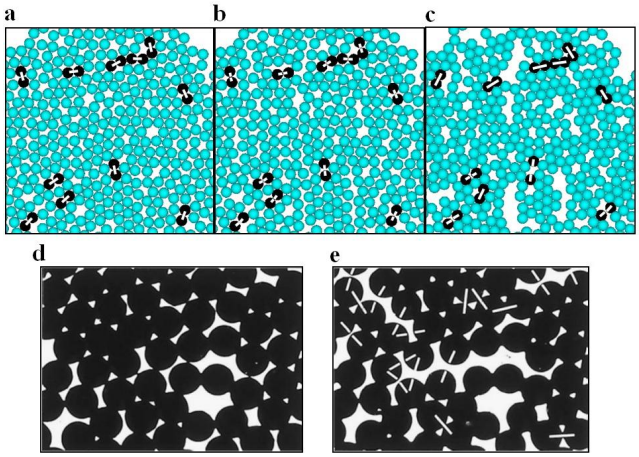

Fig. 8 Contact interface breaking and re-forming during sintering. **a**, **b**, **c** Snapshots of simulation results at three moments, initial stage, 10^5 time step, 10^6 time step, respectively; **d** and **e** Snapshots of experimental results [16] for glass spheres sintering for 1 hour and 16 hours at 1 000 K, respectively

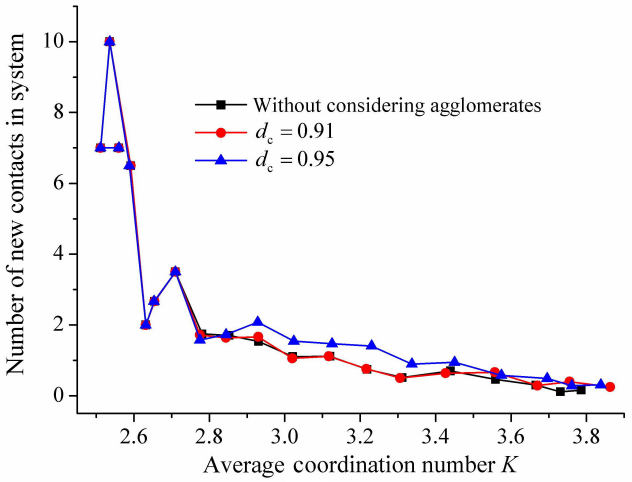

Fig. 9 The number of new forming interfaces at every 5 000 time steps varying with the average coordination number K

The result that agglomeration could enhance densification may also be verified by Fig. 10, in which the relation between the average coordination number and the densification is given. For a given average coordination number, more densification will be achieved when agglomerates are included.

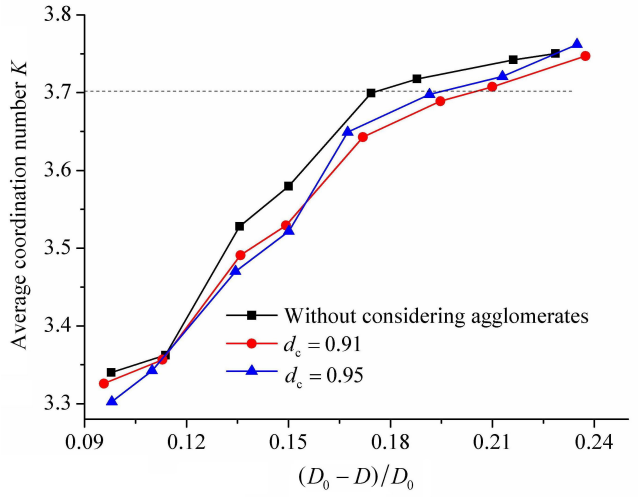

Fig. 10 Average coordination number K against the densification $(D_0 - D)/D_0$ with and without the effect of agglomerates

More obvious evidence can be found in Fig. 11, where the densification of a sintering system is shown to vary with the sintering time. At the same sintering time, it can be found that the densification of systems with the effect of agglomerates taken into consideration is significant higher than that without.

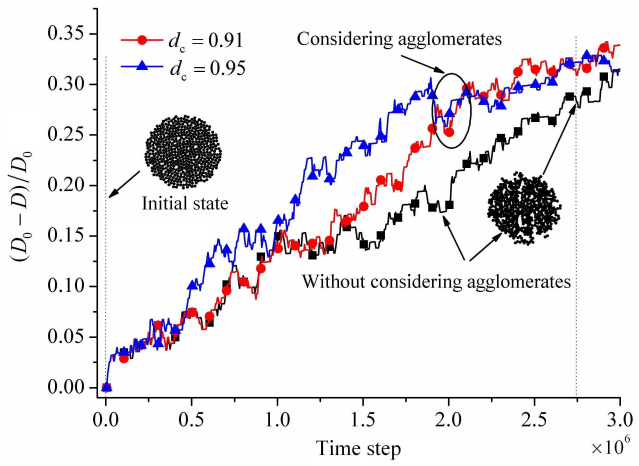

Fig. 11 The densification $(D_0 - D)/D_0$ as a function of the simulation time step with and without the effect of agglomerates

Intuitively, it seems that the pore coarsening and densification are completely opposite phenomena. In our opinion, pore coarsening is also a result of particle rearrangement and formation of agglomerates during sintering. Initially, the scattered small pores exist almost uniformly among particles. As particle rearrangement and agglomeration take place, plenty of scattered small pores will get together to form a fewer larger pores. Furthermore, a fraction of the initially total volume of pores will be occupied by particles or agglomerates, part of it will be excluded, especially for pores near the boundaries of the sintering system. With the growth of sintering time, particle coherence and agglomerates approaching each other will lead to a reduction of the few larger pores. As a result, pore coarsening happens along with an improved densification and a reduced porosity.

6 Conclusions

Not only particle rearrangement but also agglomerate rearrangement has been found in many sintering experiments [1, 17]. The effect of particle rearrangement has already been investigated in many numerical simulations [2–7, 9, 10], while the effect of agglomerate rearrangement on microstructural evolution is still kept unclear, which is the main interest of the present paper. Agglomerates do not exist initially in a particle sintering system, which will emerge spontaneously and then grow up during sintering. A definition for agglomerate is given and the effects of agglomerates on sintering are investigated using discrete element method for a planar layer of copper particles. In contrast to the case without considering the rearrangement of agglomerates, we find that agglomerates' rearrangement could improve the densification of the particle system. All the simulated phenomena agree qualitatively well with the experimental observations [1, 23]. The finding in the present paper reveals the functioning of agglomerates' rearrangement in sintering, which should be very useful for deepening the understanding of sintering process. In addition, the present model could be readily extended to three-dimensional cases for further exploring the influences of agglomerate on microstructural evolution.

References

1 Petzow, G., Exner, H.E.: Particle rearrangement in solid-state sintering. Z. Metallk. **67**, 611–618 (1976)
2 Wonisch, A., Kraft, T., Moseler, M., et al.: Effect of different particle size distributions on solid-state sintering: A microscopic simulation approach. J. Am. Ceram. Soc. **92**, 1428–1434 (2009)
3 Martin, C.L., Camacho-Montes, H., Olmos, L., et al.: Evolution of defects during sintering: discrete element simulations. J. Am. Ceram. Soc. **92**, 1435–1441 (2009)
4 Martin, C.L., Bordia, R.K.: The effect of a substrate on the sintering of constrained films. Acta Mater. **57**, 549–558 (2009)
5 Wonisch, A., Kraft, T., Moseler, M., et al.: Discrete element simulations of constrained ceramic powder sintering Ceramic forum international: CFI. Berichte der Deutschen Keramischen Gesellschaft **85**, 18–23 (2008)
6 Wonisch, A., Guillon, O., Kraft, T., et al.: Stress-induced anisotropy of sintering alumina: Discrete element modelling and experiments. Acta Mater. **55**, 5187–5199 (2007)
7 Henrich, B., Wonisch, A., Kraft, T., et al.: Simulations of the influence of rearrangement during sintering. Acta Mater. **55**, 753–762 (2007)
8 Wonisch, A., Kraft, T., Riedel, H.: Multi-scale simulations of

rearrangement effects and anisotropic behaviour during sintering. Advances in Science and Technology **45**, 530–538 (2006)
9 Martin, C.L., Schneider, L.C.R., Olmos, L., et al.: Discrete element modeling of metallic powder sintering. Scr. Mater. **55**, 425–428 (2006)
10 Parhami, F., McMeeking, R.M.: A network model for initial stage sintering. Mech. Mater. **27**, 111–124 (1998)
11 Nikolic, Z.S.: A model for 3-d study of rearrangement in liquid phase sintering. Z. Metallk. **95**, 993–1000 (2004)
12 Weiser, M.W., Dejonghe, L.C.: Rearrangement during sintering in two-dimensional arrays. J. Am. Ceram. Soc. **69**, 822–826 (1986)
13 Martin, C.L., Bouvard, D., Shima, S.: Study of particle rearrangement during powder compaction by the discrete element method. J. Mech. Phys. Solids **51**, 667–693 (2003)
14 Jagota, A., Scherer, G.W.: Viscosities and sintering rates of composite packings of spheres. J. Am. Ceram. Soc. **78**, 521–528 (1995)
15 Lange, F.F.: Sinterability of agglomerated powders. J. Am. Ceram. Soc. **67**(2), 83–89 (1984)
16 Exner, H.E., Muller, C.: Particle rearrangement and pore space coarsening during solid-state sintering. J. Am. Ceram. Soc. **92**, 1384–1390 (2009)
17 Lange, F.F., Metcalf, M.: Processing-related fracture origins. 2. Agglomerate motion and cracklike internal surfaces caused by differential sintering. J. Am. Ceram. Soc. **66**, 398–406 (1983)
18 Ciftcioglu, M., Akinc, M., Burkhart, L.: Effect of agglomerate strength on sintered density for yttria powders containing agglomerates of monosize spheres. J. Am. Ceram. Soc. **70**, C329–C334 (1987)
19 Kuo, J., Bourell, D.L.: Structural evolution during calcination of sol-gel synthesized alumina and alumina-8 vol% zirconia composite. J. Mater. Sci. **32**, 2687–2692 (1997)
20 Palmero, P., Lombardi, M., Montanaro, L., et al.: Effect of heating rate on phase and microstructural evolution during pressureless sintering of a nanostructured transition alumina. Int. J. Appl. Ceram. Technol. **6**, 420–430 (2009)
21 Martin, C.L., Bouvard, D., Delette, G.: Discrete element simulations of the compaction of aggregated ceramic powders. J. Am. Ceram. Soc. **89**, 3379–3387 (2006)
22 Kim, J.C., Auh, K.H., Martin, D.M.: Multi-level particle packing model of ceramic agglomerates. Model. Simul. Mater. Sci. Eng. **8**, 159–168 (2000)
23 Exner, H.E., Petzow, G.: Shrinkage and rearrangement during sintering of glass spheres. In: Kuczynski, G.C. ed. Sintering and Catalysis. Plenum Press Publ. Corp., New York, 279–293 (1975)
24 Claussen, N., Exner, H.E.: Influence of sintering on fine powder compacts for catalyst application. Powder Metall. **15**, 202–215 (1972)
25 Ada, K., Onal, M., Sarikaya, Y.: Investigation of the intraparticle sintering kinetics of a mainly agglomerated alumina powder by using surface area reduction. Powder Technol. **168**, 37–41 (2006)
26 Kadushnikov, R.M., Alievskii, D.M., Alievskii, V.M., et al.: Computer-simulation for microstructure evolution in a polydisperse material on sintering. 2. Zoned segregation. Sov. Powder Metall. Met. Ceram. **30**, 356–360 (1991)
27 Kadushnikov, R.M., Alievskii, D.M., Alievskii, V.M., et al.: Computer modeling of the evolution of the microstructure of polydisperse materials in sintering. 1. Principal postulates. Sov. Powder Metall. Met. Ceram. **30**, 106–111 (1991)
28 Kadushnikov, R.M., Skorokhod, V.V.: Simulating zonal segregation in powder sintering. Sov. Powder Metall. Met. Ceram. **30**, 557–561 (1991)
29 Thornton, C., Antony, S.: Quasi-static deformation of particulate media. Philos. Trans. R. Soc. A-Math. Phys. Eng. Sci. 2763–2782 (1998)
30 Thornton, C., Antony, S.J.: Quasi-static shear deformation of a soft particle system. Powder Technol. **109**, 179–191 (2000)
31 Olmos, L., Martin, C.L., Bouvard, D., et al.: Investigation of the sintering of heterogeneous powder systems by synchrotron microtomography and discrete element simulation. J. Am. Ceram. Soc. **92**, 1492–1499 (2009)
32 Cundall, P.A., Strack, O.D.L.: Discrete numerical-model for granular assemblies. Geotechnique **29**, 47–65 (1979)
33 Wang, D., Zhou, Y.: Particle dynamics in dense shear granular flow. Acta Mech. Sin. **26**, 91–100 (2010)
34 Olmos, L., Martin, C.L., Bouvard, D.: Sintering of mixtures of powders: experiments and modelling. Powder Technol. **190**, 134–140 (2009)
35 Bouvard, D., McMeeking, R.M.: Deformation of interparticle necks by diffusion-controlled creep. J. Am. Ceram. Soc. **79**, 666–672 (1996)
36 Parhami, F., McMeeking, R.M.: A network model for initial stage sintering. Mech. Mater. **27**, 111–124 (1998)
37 Braginsky, M., Tikare, V., Olevsky, E.: Numerical simulation of solid state sintering. Int. J. Solids Struct. **42**, 621–636 (2005)
38 Tikare, V., Braginsky, M., Bouvard, D., et al.: Numerical simulation of microstructural evolution during sintering at the mesoscale in a 3d powder compact. Comput. Mater. Sci. **48**, 317–325 (2010)
39 Riedel, H., Zipse, H., Svoboda, J.: Equilibrium pore surfaces, sintering stresses and constitutive equations for the intermediate and late stages of sintering–ii. Diffusional densification and creep. Acta Metallurgica et Materialia **42**, 445–452 (1994)